

# Degradation of Photopic and Mesopic Contrast Sensitivity Function in High Myopes With Partial Posterior Vitreous Detachment

Jian Zhao<sup>1,2,\*</sup>, Minzhi Xiao<sup>3,\*</sup>, Ye Zhu<sup>1,2</sup>, Qianwen Gong<sup>1,2</sup>, Jia Qu<sup>1,2</sup>, Fan Lu<sup>1,2</sup>, and Liang Hu<sup>1,2</sup>

<sup>1</sup> National Clinical Research Center for Ocular Diseases, Eye Hospital, Wenzhou Medical University, Wenzhou, China

<sup>2</sup> National Engineering Research Center of Ophthalmology and Optometry, Eye Hospital, Wenzhou Medical University, Wenzhou, China

<sup>3</sup> Department of Ophthalmology, the Second People's Hospital of Foshan, Foshan, China

**Correspondence:** Liang Hu, Eye Hospital and School of Ophthalmology and Optometry, Wenzhou Medical University, 270 Xueyuan Road, Wenzhou, Zhejiang 325027, China. e-mail: [huliang@eye.ac.cn](mailto:huliang@eye.ac.cn)

Fan Lu, Eye Hospital and School of Ophthalmology and Optometry, Wenzhou Medical University, 270 Xueyuan Road, Wenzhou, Zhejiang 325027, China. e-mail: [lufan62@mail.eye.ac.cn](mailto:lufan62@mail.eye.ac.cn)

Jia Qu, Eye Hospital and School of Ophthalmology and Optometry, Wenzhou Medical University, 270 Xueyuan Road, Wenzhou, Zhejiang 325027, China. e-mail: [qujia@eye.ac.cn](mailto:qujia@eye.ac.cn)

**Received:** November 22, 2023

**Accepted:** February 18, 2024

**Published:** April 2, 2024

**Keywords:** myopia; posterior vitreous detachment (PVD); contrast sensitivity function (CSF); ocular scatter; wavefront aberration

**Citation:** Zhao J, Xiao M, Zhu Y, Gong Q, Qu J, Lu F, Hu L. Degradation of photopic and mesopic contrast sensitivity function in high myopes with partial posterior vitreous detachment. *Transl Vis Sci Technol.* 2024;13(4):3. <https://doi.org/10.1167/tvst.13.4.3>

**Purpose:** The purpose of this study was to evaluate the effects of posterior vitreous detachment (PVD) on visual quality in patients with high myopia, as well as investigate the associated factors of photopic and mesopic contrast sensitivity function (CSF) in high myopia.

**Methods:** Visual quality was comprehensively assessed in patients with high myopia. Visual acuity, contrast sensitivity (CS) at four spatial frequencies (3, 6, 12, and 18 cycles per degree [c.p.d.]) under photopic and mesopic conditions, as well as the modulation transfer function cutoff value (MTF<sub>cutoff</sub>), the objective scatter index (OSI), the Strehl ratio (SR), and internal aberrations, were measured in this cross-sectional study.

**Results:** This study included 94 eyes from 47 subjects with bilateral high myopia, including 23 eyes with complete PVD (cPVD), 21 eyes with partial PVD (pPVD), and 50 eyes without PVD (nPVD). There was no significant difference in visual quality between the cPVD group and the nPVD group. Whereas in eyes with pPVD, there was a degradation of overall photopic CSF (versus nPVD,  $P = 0.048$ ), photopic CS at 3 c.p.d. (versus cPVD,  $P = 0.009$  and versus nPVD,  $P = 0.032$ ), photopic CS at 18 c.p.d. (versus nPVD,  $P = 0.033$ ), overall mesopic CSF (versus nPVD,  $P = 0.033$ ), and secondary astigmatism (versus cPVD,  $P = 0.044$ ). Under photopic conditions, the factors affecting CSF were pPVD and SR, whereas the factors affecting mesopic CSF were pPVD, OSI, and ganglion cell-inner plexiform layer thickness.

**Conclusions:** The pPVD impaired visual quality in patients with high myopia compared to nPVD or cPVD, and pPVD could be a factor explaining CSF at both photopic and mesopic illumination.

**Translational Relevance:** Clinicians need to closely monitor patients with high myopia with pPVD due to the potential decline in visual quality and the development of vitreo-retinal disorders.

## Introduction

Nearly one-fifth of uncorrected blindness and vision impairment worldwide is caused by refractive error, primarily myopia,<sup>1</sup> which exerts deleterious socioeconomic consequences. It is estimated that 40% of the world's population will be afflicted with myopia by 2030, and this number will grow to 50% by 2050.<sup>2,3</sup> By 2050, patients with high myopia, with a spherical equivalent refractive error  $\leq -6.00$  D,<sup>4</sup> will constitute approximately 10% of the global population.<sup>2</sup> Previous studies on the structural changes associated with myopia have been focused on the sclera, retina, choroid, etc.,<sup>5</sup> whereas the vitreous is generally less studied, in part, due to the limitations of standard imaging modalities.<sup>6</sup> Typical features of myopic vitreopathy are early fibrous vitreous liquefaction and posterior vitreous detachment (PVD).<sup>7</sup> PVD develops when the posterior vitreous cortex (PVC) separates from the inner limiting membrane (ILM).<sup>8</sup> Recent findings suggested earlier and asymmetrically progressed PVD in highly myopic eyes, as well as larger bursa premacularis in those without PVD.<sup>9-11</sup>

Currently, the most accurate way to diagnose PVD is through ultrasonography (US),<sup>12</sup> however, the diagnostic ability of US on partial PVD (pPVD) is lower than that of optical coherence tomography (OCT),<sup>13,14</sup> which exceeds in imaging the vitreoretinal interface.<sup>6,15</sup> Nevertheless, when PVC is not close enough to the retina after PVD, using OCT alone to diagnose PVD is unreliable.<sup>16</sup> A combination of US and OCT can better evaluate the overall PVD status. Recently, Mori et al. presented a more detailed PVD classification system utilizing montaged OCT images.<sup>17,18</sup> It was found that PVD begins as early as in the first decade of life, noted primarily in the paramacular-peripheral region, and gradually grows more extensive over time, which has prompted a shift in our understanding of PVD evolution. However, whether different PVD degrees affect visual function differently has not been investigated.

PVD is a critical participant in the development and progression of various vitreoretinal disorders, and it is thought to be the most common cause of symptomatic vitreous floaters.<sup>19</sup> Several studies have shown that PVD can reduce contrast sensitivity function (CSF),<sup>7,20-22</sup> most likely as a result of increased light scattering induced by the dense collagen matrix of the PVC, posterior vitreous surface folding, and possibly portions of the inner ILM that separated from the retina and remained attached to the posterior vitreous following PVD. However, the subjects in these studies were predominantly middle-

aged and older. Potential confounding factors (age-related ocular changes) were not sufficiently controlled for. No previous study has investigated the impact of myopic PVD on visual quality in patients with high myopia younger than age 40 years, who have increased visual demands during daily activities.

Patients with symptomatic PVD seek professional help as soon as their quality of vision and life is impaired, whereas asymptomatic patients are more likely to be unaware of the presence of PVD. If left untreated, pPVD may progress to retinal tears and retinal detachment,<sup>6</sup> severely affecting the quality of life. During pre-operative examinations at our refractive surgery center, asymptomatic PVD was not uncommon in young patients with high myopia. This study set out to comprehensively evaluate visual quality (visual acuity, contrast sensitivity, objective scatter index, internal aberration, etc.) in refractive surgery candidates with different PVD statuses in order to gain a better understanding of whether myopic PVD compromises visual quality in these patients.

## Methods

### Study Design and Subjects

Approval for this study was obtained from the Ethics Committee of the Eye Hospital of Wenzhou Medical University, Wenzhou, China (2021-120-K-102). This study followed the ethical criteria outlined in the Helsinki Declaration. The subjects agreed to participate after a detailed explanation of the study's purpose and possible consequences. Subject data were prospectively collected at the Eye Hospital's Refractive Surgery Center. Eyes with high myopia were categorized based on the presence or absence of PVD, then a subgroup analysis was conducted, further dividing PVD into pPVD and complete PVD (cPVD; definitions seen below). This study excluded eligible refractive surgery patients with high myopia worse than  $-10.00$  diopters (D) to reduce the presence of posterior staphyloma or myopic maculopathy, as the risk of pathologic myopia increases with the degree of myopia.<sup>23</sup>

Inclusion criteria were patients with pre-operative ages between 17 and 40 years; spherical equivalent between  $-6.00$  and  $-10.00$  diopters (D), astigmatism less than 3.00 D; best corrected visual acuity greater than 0.05 log MAR; refractive status stable for 2 years; myopic maculopathy no worse than category 1<sup>24</sup>; and no prior experience of floaters. All patients stopped wearing soft contact lenses for at least 2 weeks, rigid contact lenses for at least 1 month, and orthokeratology lenses for at least 3 months. After comprehensive

ophthalmic examinations, all patients were determined to be suitable candidates for myopic laser vision correction or implantable collamer lens implantation.

Patients were excluded if they had irregular astigmatism, keratoconus, or corneal dystrophy; active eye disease, such as conjunctivitis, keratitis, and uveitis; lens opacification, including posterior subcapsular cataracts, and cortical and nuclear opacification; symptomatic floaters, and anomalous, and asymmetrical PVD<sup>6,11</sup>; evidence of neural, developmental or retinal disorders, such as optic nerve damage, amblyopia, dome-shaped macula, macular neovascularization, retinoschisis, and tilted disc syndrome with inferior staphyloma; and history of trauma or surgery to the eye. In addition, patients with metabolic disorders, cardio-cerebral vascular system diseases, nervous system diseases, and other systemic conditions considered inappropriate were excluded from the study.

## Measurements

### Evaluation of Visual Quality

The Chinese standard logarithm visual chart was used to evaluate corrected distance visual acuity (CDVA), which was then converted into a log MAR unit. Manifest refraction spherical equivalent (MRSE) was calculated based on the results of cycloplegic refraction. A distance grating chart with internal retro illumination (CSV-1000E; Vector Vision, Greenville, OH, USA) was used to test contrast sensitivity (CS) at four spatial frequencies (3, 6, 12, and 18 cycles per degree [c.p.d.]) under photopic (85 c.d./m<sup>2</sup>) and mesopic (3 c.d./m<sup>2</sup>) conditions.<sup>25,26</sup> During measurement, eyes were best corrected. Patients wore a neutral density filter for the mesopic CSF testing, which delivers a testing luminance level of 3 c.d./m<sup>2</sup> after brief dark adaptation.<sup>27</sup> CSF curves were plotted over four spatial frequencies. The area under the logarithm of the CSF (AULCSF) was calculated as described previously<sup>28</sup> to determine the overall CSF. A double-pass optical quality analysis system (OQAS II; Visiometrics, Terrassa, Spain) with a 4-mm pupil diameter was used to measure the objective scatter index (OSI), the cutoff value of the modulation transfer function (MTF<sub>cutoff</sub>), and the Strehl ratio (SR). During double-pass imaging, the OSI compares the light intensity within the central 1 arc minute with the peripheral PSF of 12 and 20 arc minutes, indicating the level of intraocular scattering and overall opacity of the eye. The MTF<sub>cutoff</sub> is the cutoff value of the modulation transfer function, and SR is the ratio between the area under the modulation transfer function curve of a tested eye and that of an ideal optical system.<sup>29</sup> Tested eyes with higher MTF<sub>cutoffs</sub>,

higher SRs, and lower OSIs had better optical quality in general. These parameters evaluate intraocular scattering and retinal image quality. With the subject covered with a black cloth, a ray tracing system (iTrace; Tracey Technologies, Houston, TX, USA) with a 6-mm pupil diameter was used to analyze intraocular wavefront aberrations, including internal lower order aberrations (LOAs; defocus and astigmatism) and higher order aberrations (HOAs; coma, spherical, secondary astigmatism, and trefoil). To ensure accuracy and repeatability, measurements were carried out by well-trained ophthalmologists.

### Factors Affecting Contrast Sensitivity

To control for the potential effect of confounders on contrast sensitivity, we included relevant parameters, such as age, MRSE, axial length, pupil diameter, average ganglion cell-inner plexiform layer (GCIPL-avg) thickness, average macular choroidal thickness (MCT-avg), and OSI. Axial length was measured using an optical low-coherence reflectometry biometer (Lenstar LS 900; Haag-Streit AG, Koeniz, Switzerland). Under dim light conditions, pupil diameter was obtained from the iTrace aberrometer without mydriatic eye drops. GCIPL-avg was measured because subjects with impaired CSF were previously identified as having significant thinning in ganglion cell complex (GCC),<sup>30</sup> and because the potential sensitivity of GCIPL thickness for detecting abnormal alterations could be higher when compared to GCC as a whole.<sup>31</sup> A commercial swept-source (SS) OCT device (VG100D; SVision Imaging, Ltd., Luoyang, China) was used for the measurement of GCIPL-avg and MCT-avg. The device consisted of an SS laser (central wavelength 1050 nm; scanning rate 200,000 A-scans per second; axial resolution 5 μm; lateral resolution 13 μm; and scan depth 3 mm) and an integrated confocal scanning laser ophthalmoscope to eliminate artifacts caused by eye movement.<sup>32</sup> OCT and OCT angiography (OCTA) data were obtained with a raster scan protocol of 512 (horizontal) × 512 (vertical) B-scans (12 × 12 mm centered on the fovea). GCIPL thickness was measured at 6 locations within the papillo-macular bundle and the GCIPL-avg was calculated using an automatic algorithm, whereas MCT-avg was measured in the 1 mm, 3 mm, and 6 mm circular regions.

### Evaluation of Posterior Vitreous Detachment

The degree of PVD was assessed using the SS-OCT and an ultrasonic B scanner (UD-8000; Tomey Corp., Nagoya, Japan; Fig. 1) according to the examination and grading criteria of Moon et al.<sup>7,13</sup> Ultrasonography (US) with a 15 MHz focused probe was utilized to evaluate vitreous body status and to detect PVC when

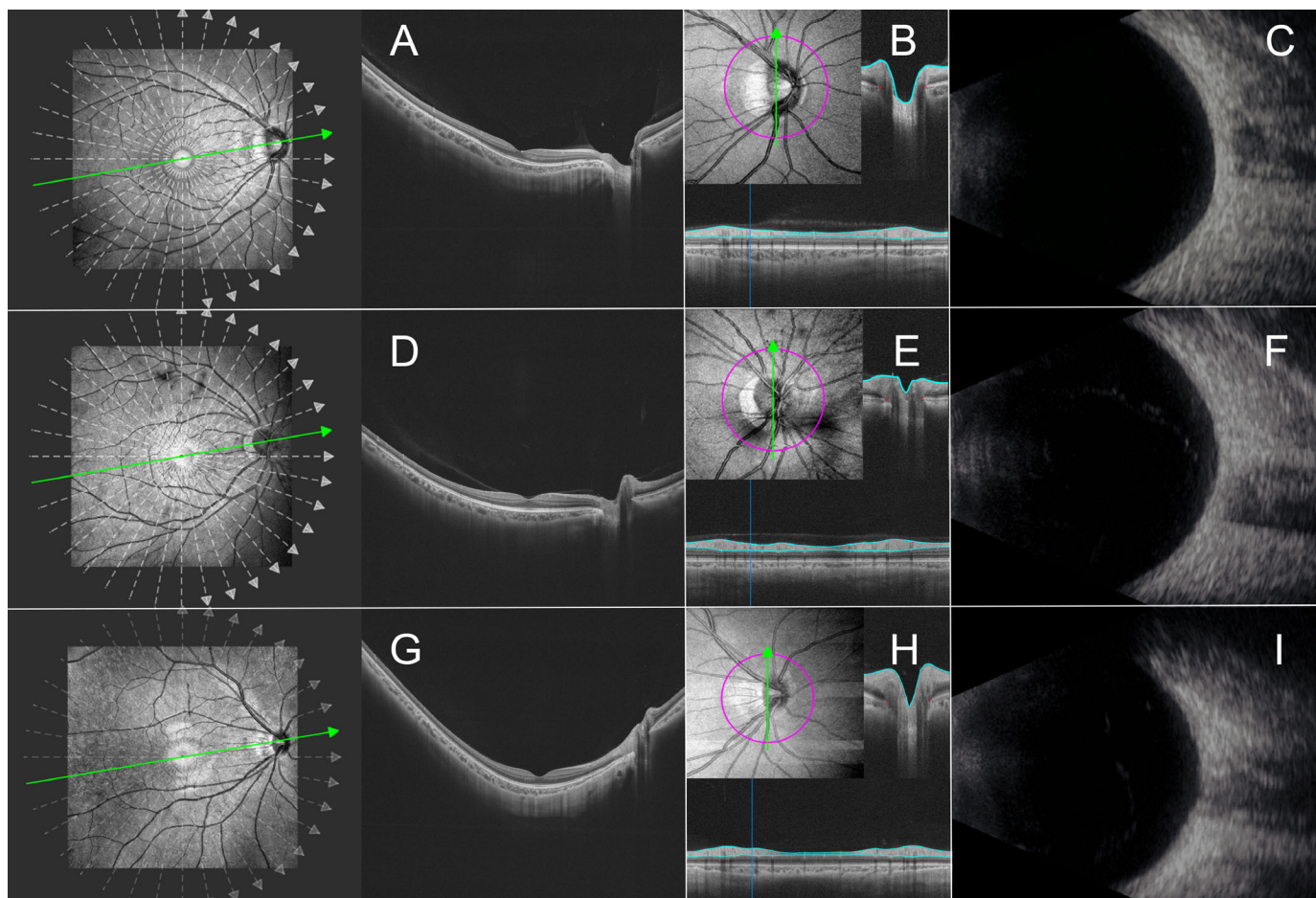


**Figure 1.** Representative graphs showing different degrees of posterior vitreous detachment (PVD) in high myopes based on swept-source optical coherence tomography (SS-OCT) and ultrasonography (US). (**A–C**) No PVD, (**D–F**) partial PVD, and (**G–I**) complete PVD. In patients with high myopia without PVD, (**A**) the posterior vitreous cortex (PVC) is completely attached to the retina and the bursa premacularis is evident. (**B**) Peripapillary scan displays a highly reflective membrane attached to the peripapillary retina. (**C**) No hyperechoic membrane is observed over the retinal pigment epithelium (RPE) layer on US. In patients with high myopia with partial PVD, (**D**) the detached PVC is observable within 2500  $\mu\text{m}$  of the parafoveal area. (**E**) Peripapillary scan also reveals a highly reflective membrane attached to the peripapillary region. (**F**) US demonstrates a hyperechoic membrane partially detached from the posterior retina. In patients with high myopia with complete PVD, (**G**) the PVC is not observable in either macular or optic disc region. (**H**) Peripapillary scan shows no highly reflective membrane attached to the peripapillary retina. (**I**) US shows a hyperechoic membrane completely detached from the posterior retina.

it is positioned far anteriorly from the fundus. When the PVC was close to the fundus, SS-OCT was used to confirm PVD, and to rule out substantial myopic maculopathy and myopia-associated optic neuropathy. Then, 18 radial scan lines (12 mm in length) were used for structural OCT centered on the fovea. PVD status was determined using a single image traversing both the optic disc and fovea. Additional optic nerve head (ONH) imaging was performed using  $6 \times 6$  mm scans to evaluate peripapillary vitreous status. No PVD (nPVD) was defined on SS-OCT, as complete attachment of the PVC to the fovea and optic disc, including the perifoveal, parafoveal, and peripapillary areas. PVD outside the parafoveal area (2500  $\mu\text{m}$  in diameter) was also classified as nPVD; pPVD specifically referred

to detached PVC within the parafoveal area (2500  $\mu\text{m}$  in diameter), with PVC attached to the peripapillary retina; and cPVD was defined as no apparent attached PVC in the macula, optic disc and the peripapillary area. In US, nPVD was defined with absence of a hyperechoic membrane over the retina; pPVD was defined when a hyperechoic membrane separated from the posterior retina, but part of the membrane is still attached to the retinal pigment epithelium (RPE) layer; and cPVD was defined when a hyperechoic membrane is apart from the retina and fully detached from the RPE layer. PVD status was assessed by two independent evaluators (authors J.Z. and M.X.). If the grading results were inconsistent, the images were reviewed and re-assessed collectively. Based on the US and OCT

findings, the two evaluators reached a final agreement of the patient's PVD status. In general, when assessing whether there was pPVD, the OCT findings were used, whereas the US findings were used to determine whether there is complete or no PVD.<sup>13</sup>

### Statistical Analysis and Sample Size Calculation

Statistical analysis was performed using SPSS (26.0; IBM Corp, Armonk, NY, USA), and the data are presented using range and mean  $\pm$  standard deviation. The normality of the data distributions was examined using the Shapiro-Wilk test and by visual inspection of frequency histograms. Comparisons of demographic and clinical characteristics were performed using generalized estimating equations (GEEs), and Bonferroni correction was applied to multiple comparisons. GEEs were also used in all subjects to assess the correlation between variables. Significant variables were included in the final equations and collinearity was investigated. This analysis used both eyes of each subject, and the inter-eye correlation was adjusted by GEEs. At  $P < 0.05$ , the results were considered statistically significant.

PASS software (15.0; NCSS, Kaysville, UT, USA) was used to calculate the sample size. Utilizing the mesopic AULCSF from 30 eyes obtained in our preliminary investigation, it was determined that at least 36 nPVD, 6 pPVD, and 18 cPVD eyes were required in each group. Using an F test with a 0.05 significance level, the total sample of 60 eyes achieved 97% power to detect differences between means against the alternative of equal means. The size of the variation in the means was represented by their standard deviation, which was 0.03.

## Results

This study was carried out between July 2021 and September 2022. Ninety-four eyes from 47 young adults (21 men and 26 women) with bilateral high myopia were included, and these eyes were grouped into the nPVD group ( $n = 50$ ) and the PVD group ( $n = 44$ ). Eyes with PVD were further grouped into the pPVD group ( $n = 21$ ) and the cPVD group ( $n = 23$ ). As shown in Table 1 and Supplementary Table S1,

**Table 1.** Demographic Characteristics of Study Participants

Variables	nPVD ( $n = 50$ )	pPVD ( $n = 21$ )	cPVD ( $n = 23$ )	Sig.
Sex, male/female	22/28	6/15	14/9	0.239
Age, years	24.00 $\pm$ 3.87 17 ~ 32	26.24 $\pm$ 4.45 19 ~ 32	23.61 $\pm$ 6.17 18 ~ 36	0.233
MRSE, D	-7.92 $\pm$ 1.19	-8.21 $\pm$ 1.06	-8.58 $\pm$ 1.50	0.320
Axial length, mm	26.70 $\pm$ 1.04 24.62 ~ 28.51	26.69 $\pm$ 1.03 24.68 ~ 29.64	26.90 $\pm$ 1.03 25.40 ~ 28.95	0.835
Pupil diameter, mm	7.05 $\pm$ 0.45 6.17 ~ 7.96	6.97 $\pm$ 0.37 6.25 ~ 7.87	7.12 $\pm$ 0.47 6.25 ~ 8.00	0.637
CDVA, log MAR	-0.02 $\pm$ 0.04 -0.08 ~ 0.05	-0.01 $\pm$ 0.03 -0.08 ~ 0.05	-0.02 $\pm$ 0.04 -0.08 ~ 0.05	0.273
GCIPL-avg, $\mu$ m	71.93 $\pm$ 6.58 58.28 ~ 86.91	71.33 $\pm$ 7.41 54.33 ~ 84.66	69.51 $\pm$ 5.38 59.64 ~ 77.47	0.434
MCT-avg, $\mu$ m				
0-1 mm	236.23 $\pm$ 78.03 105.39 ~ 457.40	227.53 $\pm$ 61.96 124.47 ~ 370.69	201.51 $\pm$ 61.77 143.08 ~ 425.89	0.181
0-3 mm	237.41 $\pm$ 74.71 116.36 ~ 459.60	225.20 $\pm$ 53.49 131.50 ~ 362.85	202.75 $\pm$ 56.35 151.11 ~ 404.45	0.148
0-6 mm	238.86 $\pm$ 66.91 135.49 ~ 448.58	229.05 $\pm$ 51.13 156.47 ~ 362.13	209.41 $\pm$ 48.51 157.29 ~ 375.74	0.174

CDVA, corrected distance visual acuity; cPVD, complete posterior vitreous detachment; GCIPL-avg, average ganglion cell-inner plexiform layer thickness; MCT-avg, average macular choroidal thickness; MRSE, manifest refraction spherical equivalent; nPVD, no posterior vitreous detachment; pPVD, partial posterior vitreous detachment; Sig., the statistical difference between groups.

\*Statistically significant difference between groups at the 0.05 level.

**Table 2.** Impact of Posterior Vitreous Detachment on Visual Quality in Patients With High Myopia

Variables	nPVD (n = 50)	pPVD (n = 21)	cPVD (n = 23)	Sig.
Photopic AULCSF	1.074 ± 0.108 0.774 ~ 1.336	1.012 ± 0.089 0.873 ~ 1.225	1.074 ± 0.124 0.757 ~ 1.242	0.041*
CS at f3	1.719 ± 0.102 1.49 ~ 1.94	1.645 ± 0.106 1.44 ~ 1.84	1.753 ± 0.123 1.49 ~ 1.99	0.007*
CS at f6	1.831 ± 0.166 1.38 ~ 2.30	1.769 ± 0.135 1.55 ~ 2.00	1.819 ± 0.169 1.44 ~ 2.10	0.193
CS at f12	1.367 ± 0.269 0.61 ~ 2.00	1.310 ± 0.211 0.91 ~ 1.70	1.296 ± 0.282 0.61 ~ 1.75	0.540
CS at f18	0.852 ± 0.215 0.27 ~ 1.31	0.729 ± 0.191 0.17 ~ 1.16	0.838 ± 0.255 0.12 ~ 1.16	0.035*
Mesopic AULCSF	0.655 ± 0.240 0.259 ~ 1.096	0.490 ± 0.187 0.259 ~ 0.884	0.686 ± 0.270 0.325 ~ 1.122	0.019*
CS at f3	1.599 ± 0.172 1.17 ~ 1.94	1.549 ± 0.184 1.11 ~ 1.79	1.649 ± 0.157 1.34 ~ 1.99	0.285
CS at f6	1.502 ± 0.219 1.01 ~ 1.90	1.372 ± 0.274 0.81 ~ 1.95	1.470 ± 0.299 0.81 ~ 2.00	0.301
CS at f12	0.817 ± 0.305 0.31 ~ 1.55	0.695 ± 0.250 0.31 ~ 1.19	0.818 ± 0.335 0.31 ~ 1.85	0.292
CS at f18	0.370 ± 0.305 0.01 ~ 1.26	0.260 ± 0.265 0.01 ~ 0.96	0.340 ± 0.269 0.01 ~ 0.75	0.348
OSI	1.299 ± 0.853 0.30 ~ 4.03	1.335 ± 0.939 0.37 ~ 4.53	1.312 ± 0.917 0.40 ~ 3.93	0.992
MTF cutoff	32.719 ± 9.519 12.503 ~ 50.125	34.286 ± 8.531 19.707 ~ 51.045	36.441 ± 9.647 19.435 ~ 49.355	0.410
SR	0.179 ± 0.053 0.089 ~ 0.300	0.186 ± 0.044 0.107 ~ 0.269	0.191 ± 0.051 0.104 ~ 0.284	0.685
Total internal aberration, μm	10.910 ± 1.540 7.461 ~ 13.886	10.951 ± 1.114 9.206 ~ 13.197	11.260 ± 1.799 7.116 ~ 14.473	0.823
Total internal LOA, μm	10.875 ± 1.528 7.449 ~ 13.830	10.917 ± 1.115 9.184 ~ 13.175	11.219 ± 1.779 7.104 ~ 14.406	0.826
Defocus, μm	10.743 ± 1.480 7.431 ~ 13.640	10.827 ± 1.128 9.080 ~ 13.088	11.068 ± 1.748 7.001 ~ 14.345	0.840
Astigmatism, μm	1.514 ± 0.814 0.337 ~ 3.783	1.263 ± 0.566 0.314 ~ 2.724	1.700 ± 0.737 0.940 ~ 3.269	0.122
Total internal HOA, μm	0.838 ± 0.277 0.327 ~ 1.522	0.832 ± 0.164 0.535 ~ 1.209	0.916 ± 0.363 0.338 ~ 1.642	0.714
Coma, μm	0.367 ± 0.189 0.110 ~ 0.958	0.353 ± 0.138 0.109 ~ 0.600	0.453 ± 0.201 0.090 ~ 0.820	0.173
Spherical, μm	0.195 ± 0.162 -0.257 ~ 0.559	0.198 ± 0.191 -0.280 ~ 0.419	0.272 ± 0.210 -0.106 ~ 0.611	0.483
Secondary astigmatism, μm	0.256 ± 0.097 0.119 ~ 0.516	0.278 ± 0.086 0.149 ~ 0.481	0.196 ± 0.117 0.055 ~ 0.480	0.046*
Trefoil, μm	0.447 ± 0.266 0.071 ~ 1.211	0.446 ± 0.212 0.153 ~ 0.886	0.483 ± 0.292 0.124 ~ 1.176	0.886

AULCSF, area under the logarithm of the CSF; cPVD, complete posterior vitreous detachment; CS at f3, contrast sensitivity at spatial frequency of 3 c.p.d.; HOA, higher order aberration; LOA, lower order aberration; MTF cutoff, cutoff value of the modulation transfer function; nPVD, no posterior vitreous detachment; OSI, ocular scatter index; pPVD, partial posterior vitreous detachment; Sig., the statistical difference between groups; SR, Strehl ratio.

\*Statistically significant difference between groups at the 0.05 level.

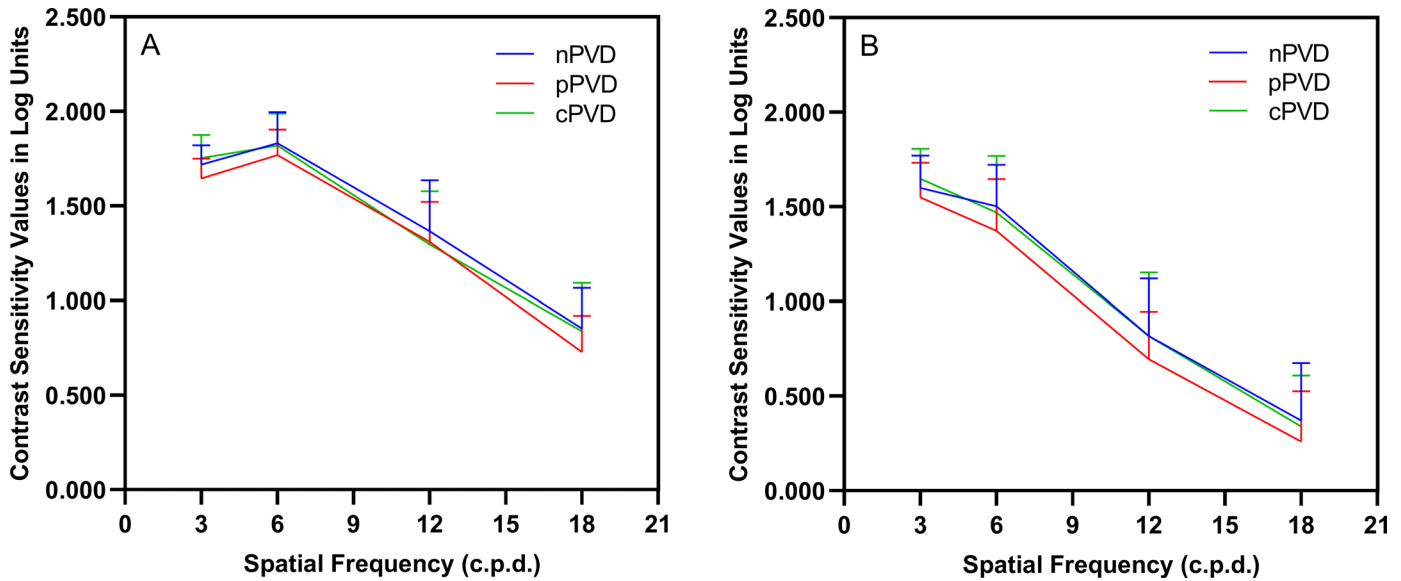


**Figure 2.** Contrast sensitivity curves in patients with high myopia with different posterior vitreous detachment (PVD) status under photopic (A) and mesopic (B) conditions (c.p.d. = cycles per degree; nPVD = no posterior vitreous detachment; pPVD = partial posterior vitreous detachment; cPVD = complete posterior vitreous detachment).

demographic characteristics do not differ significantly among the groups.

### Impact of Posterior Vitreous Detachment on Visual Quality in High Myopes

Supplementary Table S2 demonstrates visual quality parameters in patients with high myopia with and without PVD. There were no differences observed among the groups in terms of any visual quality parameters. Table 2 demonstrates visual quality parameters in patients with high myopia with different PVD statuses (nPVD, pPVD, and cPVD). Figure 2 exhibits the contrast sensitivity curves for the three groups at two conditions. The photopic AULCSF differed significantly among the three groups ( $P = 0.041$ ; Fig. 3A); specifically, photopic CSF was worse in pPVD eyes compared with nPVD ( $P = 0.048$ ) but was not significantly different between the pPVD group and the cPVD group ( $P = 0.244$ ), the nPVD group, and the cPVD group ( $P = 1.000$ ). The photopic CS at 3 c.p.d. showed a significant difference ( $P = 0.007$ ; Fig. 3B); specifically, CS was worse in pPVD eyes compared with nPVD ( $P = 0.032$ ) or cPVD ( $P = 0.009$ ), and there was no difference between the nPVD group and the cPVD group ( $P = 0.790$ ). The photopic CS at 18 c.p.d. showed a significant difference ( $P = 0.035$ ; Fig. 3C); specifically, CS was worse in pPVD eyes compared with nPVD eyes ( $P = 0.033$ ) but was not

significantly different between the pPVD group and the cPVD group ( $P = 0.396$ ), the nPVD group, and the cPVD group ( $P = 1.000$ ). The mesopic AULCSF was also significantly different among groups ( $P = 0.019$ ; Fig. 3D); mesopic CSF was worse in pPVD eyes compared with nPVD eyes ( $P = 0.033$ ) but was not significantly different between the pPVD group and the cPVD group ( $P = 0.086$ ), the nPVD group, and the cPVD group ( $P = 1.000$ ). No statistical difference was found between groups for OSI ( $P = 0.992$ ), MTFcutoff ( $P = 0.410$ ), and SR ( $P = 0.685$ ). As for internal aberrations, secondary astigmatism was found to differ significantly among the three groups ( $P = 0.046$ ; Fig. 3E); in particular, the pPVD group had higher secondary astigmatism compared with the cPVD group ( $P = 0.044$ ), whereas there was no significant difference between the nPVD group and the pPVD group ( $P = 1.000$ ), the nPVD group, and the cPVD group ( $P = 0.151$ ). No significant difference was observed in terms of other aberrations.

### Factors Correlated With Contrast Sensitivity Function

Age, MRSE, axial length, pupil diameter, CDVA, GCIPL-avg, MCT-avg, OSI, and SR were selected as independent variables. Table 3 shows the results of the significant variables in two GEE models. In comparison to nPVD, pPVD demonstrated a significant corre-

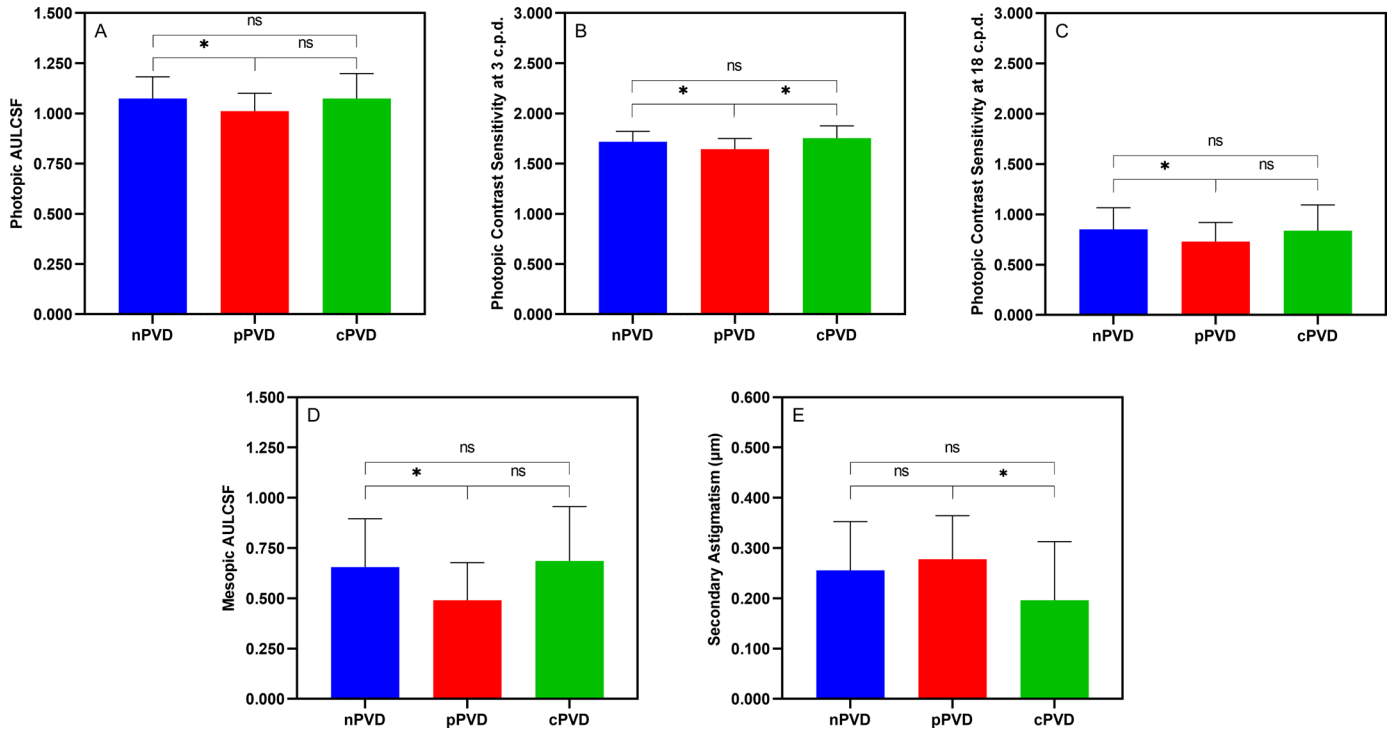


**Figure 3.** Comparisons of photopic AULCSF (A), photopic contrast sensitivity at 3 c.p.d. (B), photopic contrast sensitivity at 18 c.p.d. (C), mesopic AULCSF (D), and internal secondary astigmatism (E) between groups (AULCSF = area under the logarithm of the CSF; c.p.d. = cycles per degree; nPVD = no posterior vitreous detachment; pPVD = partial posterior vitreous detachment; cPVD = complete posterior vitreous detachment; ns = no significant difference; \*, statistically significant difference between groups at the 0.05 level).

**Table 3.** Factors Correlated With Contrast Sensitivity Function

AULCSF at Photopic Illumination			AULCSF at Mesopic Illumination		
Variables	$\beta$	Sig.	Variables	$\beta$	Sig.
Intercept	0.989	<0.001*	Intercept	0.147	0.588
nPVD	Reference	—	nPVD	Reference	—
pPVD	-0.065	0.009*	pPVD	-0.149	0.018*
cPVD	-0.005	0.886	cPVD	0.060	0.421
SR	0.475	0.024*	GCIPL-avg	0.008	0.025*
			OSI	-0.070	0.005*

AULCSF, area under the logarithm of the contrast sensitivity function; nPVD, no posterior vitreous detachment; pPVD, partial posterior vitreous detachment; cPVD, complete posterior vitreous detachment; SR, Strehl ratio; GCIPL-avg, average ganglion cell-inner plexiform layer thickness; OSI, ocular scatter index;  $\beta$ , partial regression coefficient; Sig., the statistical difference.

\*Statistically significant at the 0.05 level.

lation with photopic AULCSF ( $\beta = -0.065$ ,  $P = 0.009$ ), whereas cPVD did not ( $\beta = -0.005$ ,  $P = 0.886$ ). SR was also found to have a positive correlation with photopic AULCSF ( $\beta = 0.475$ ,  $P = 0.024$ ). The pPVD ( $\beta = -0.149$ ,  $P = 0.018$ ), GCIPL-avg ( $\beta = 0.008$ ,  $P = 0.025$ ), and OSI ( $\beta = -0.070$ ,  $P = 0.005$ ) demonstrated a significant correlation with AULCSF in the mesopic conditions.

## Discussion

To the best of our knowledge, this is the first study to examine the impact of myopic PVD on visual quality multidimensionally in patients with high myopia younger than 40 years. In previous studies that investigated the effect of PVD on CSF in older popula-



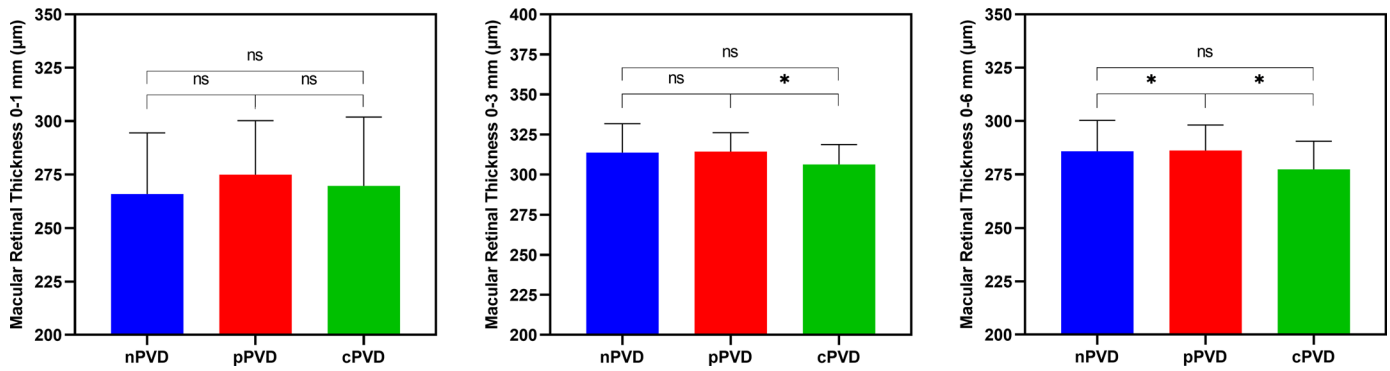


**Figure 4.** Comparisons of macular retinal thickness (0-1 mm, 0-3 mm, and 0-6 mm) between different types of PVD (nPVD = no posterior vitreous detachment; pPVD = partial posterior vitreous detachment; cPVD = complete posterior vitreous detachment; ns = no significant difference; \*, statistically significant difference between groups at the 0.05 level).

tions,<sup>7,20–22</sup> it was difficult to account for confounding factors such as aging and age-related ocular abnormalities, which are known to reduce CSF.<sup>33</sup> In addition, the PVD status has not been classified into nPVD, pPVD, and cPVD. This study, on the other hand, focused on refractive surgery candidates with high myopia and varying PVD status. The findings of this study suggest that myopic pPVD, even without symptoms, can cause significant degradation of CSF and internal secondary astigmatism when compared with nPVD or cPVD.

CDVA did not differ between groups (see Table 1, Supplementary Table S1). There were no significant differences in photopic and mesopic CSF, as well as other visual quality parameters, between groups with and without PVD (see Supplementary Table S2), however, further subgroup analysis showed that pPVD had lower overall photopic and mesopic CSF than nPVD (see Fig. 3). This could be because of the mild tractional force on the macula from an incompletely detached PVC, even though vitreomacular traction (VMT) had not yet occurred. To test this hypothesis, intergroup comparisons of macular retinal thickness were conducted among the three subgroups. It was found that the macular retinal thickness in the pPVD group was thicker within the 0 to 3 mm and 0 to 6 mm ranges compared to the other groups, and this difference was statistically significant (Fig. 4). These findings align with the previous research conducted by Shao et al.,<sup>34</sup> suggesting that the traction between the PVC and ILM in VMT can result in retinal stretching, leading to an elevation in the measured thickness on OCT.

Similar to the findings of this study, Ankamah et al.<sup>35</sup> discovered that in subjects with vitreous degeneration, CSF on both photopic and mesopic contrast thresholds did not differ significantly between eyes with cPVD and nPVD. The study investigated older subjects with bothersome floaters, for whom vitreous opac-

ities may have become too severe to render the effect of cPVD nonsignificant. Whereas our study did not involve patients with symptomatic floaters, the comparable visual quality between the nPVD and cPVD groups suggests that the absence of vitreous traction in both groups may account for this lack of significant difference. Garcia et al.<sup>20</sup> prospectively assessed the effect of cPVD on CSF in previously normal eyes and observed a reduction in mesopic CSF following cPVD. The same group analyzed the determinants of mesopic CSF and found that cPVD caused a decrease in CSF that worsened with increasing age.<sup>21</sup> In contrast, our study found similar CSF between eyes with nPVD and cPVD, suggesting that CSF might be restored following complete detachment of the PVC. When comparing the results of this study with previous research findings, it is important to exercise caution. Previous studies have primarily focused on older subjects with symptomatic PVD or floaters, in which the age-related consolidation of the pre-macular vitreous has been identified as a key mechanism contributing to the decline in visual quality. Additionally, variations in study designs could also account for differences in results.

However, the decline in visual quality in the pPVD subgroup may be the result of multiple mechanisms acting in conjunction. Another possible mechanism is the consolidation of pre-macular vitreous due to high myopia. Although no significant differences were observed among the three groups in terms of most objective visual quality parameters, indicating similar levels of intraocular light scattering, the consolidation of pre-macular vitreous can account for the relatively fewer visual quality differences between pPVD and cPVD compared to pPVD and nPVD. Secondary astigmatism was the only objective visual quality metric that differed between pPVD and cPVD, and it was previously shown to be the most detrimental to reading in

terms of internal aberrations.<sup>36</sup> Thus, reading performance could be compromised in patients with high myopia and pPVD, which warrants further validation.

No significant correlation was observed between PVD subtypes and CDVA (Supplementary Table S3), indicating that PVD may not be a determining factor for CDVA. However, pPVD was found to influence both photopic and mesopic CSF in young patients with high myopia (see Table 3). CSF decline is generally attributed to optical and neural factors.<sup>35</sup> From a neurological standpoint, the tractional stress to the macular GCC may be the primary contributor to the impaired CSF in pPVD.<sup>37</sup> In this study, other influencing factors of CSF included SR under photopic conditions and GCIPL-avg, and OSI under mesopic conditions. SR had a positive correlation with CSF. A higher SR reflects fewer aberrations present in the optical system,<sup>38</sup> hence a better outcome in CSF. OSI correlated negatively with CSF, confirming that increased intraocular light scatter plays a role in CSF decline.<sup>19,21</sup> Consistent with previous studies,<sup>30,39</sup> GCIPL-avg had a positive correlation with CSF, implying that macular GCC thinning likely due to ganglion cell loss in high myopia contributed to CSF diminution. SR and OSI therefore could be optical factors driving CSF decline, and GCIPL-avg be a neural factor.

Among the factors influencing mesopic and photopic CSF in this study, pPVD was consistent, whereas other factors varied. The differences in correlation results may be attributed to the inherent dissociation between photopic and mesopic CS. In mesopic conditions, there is a shift in the point of regard from central foveal vision to a few degrees perifoveally; additional aberrations may be introduced because of pupil enlargement; and the accommodation tends to adjust toward the individual's resting postures.<sup>40</sup> In addition, in mesopic and photopic conditions, there is a difference in the proportion of photoreceptor cells that are primarily relied upon. This leads to distinct perceptions of spatial frequency and contrast between the two conditions. These factors collectively explain the degradation of CSF in mesopic conditions (see Fig. 2).

There were some limitations to this study. Quantitative ultrasonography was not used to evaluate vitreous opacities, which had been linked to CSF.<sup>6,19</sup> Another limitation was that this study did not observe the longitudinal variations in visual quality in pPVD. Besides, vision is a dynamic process, and bright ambient illumination is thought to be detrimental to vision in patients with floaters.<sup>6</sup> Future studies may focus on dynamic visual acuity and CSF in individuals with myopic vitreopathy under varied levels of glare to simulate real-world scenarios. Last, it should be noted that the

presence of vitreous traction, if any, could have been confirmed through the Amsler chart.

In conclusion, pPVD with persistent attachment to the parafoveal macula reduced visual quality in high myopes compared to nPVD and cPVD, likely due to vitreous traction and consolidation of pre-macular vitreous. In eyes with high myopia, pPVD could explain CSF at both photopic and mesopic illumination. Refractive surgeons and eye care providers in general need to pay more attention to the different PVD statuses in young patients with high myopia due to the potential decline in visual quality, and, more importantly, explore prevention and control measures to reduce the incidence of high myopia and its associated complications.

## Acknowledgments

Supported by the Zhejiang Key Research and Development Project (2023C03106) and Wenzhou Social Development (Health Care) Science and Technology Project (ZY2020010). The authors sincerely thank all participants who enrolled in the study.

**Authors' Contributions:** Conception and design of the work was conducted by J.Z., M.X., F.L., J.Q., and L.H. Data acquisition and analysis was conducted by J.Z., M.X., and Q.G. Data interpretation was conducted by J.Z., M.X., Q.G., Y.Z., F.L., J.Q., and L.H. Manuscript writing was done by J.Z. and M.X. Manuscript review was conducted by Q.G., Y.Z., F.L., J.Q., and L.H. All authors made final approval of the version to be published and agreed to be accountable for all aspects of the work.

**Data Availability:** The data that support the findings of this study are available from the corresponding authors (L.H., F.L., and J.Q.) upon reasonable request.

**Disclosure:** J. Zhao, None; M. Xiao, None; Y. Zhu, None; Q. Gong, None; J. Qu, None; F. Lu, None; L. Hu, None

\* JZ and MX contributed equally to this work as the co-first authors.

## References

1. Flaxman SR, Bourne RRA, Resnikoff S, et al. Global causes of blindness and distance vision impairment 1990-2020: a systematic

- review and meta-analysis. *Lancet Glob Health*. 2017;5(12):e1221–e1234.
2. Holden BA, Fricke TR, Wilson DA, et al. Global prevalence of myopia and high myopia and temporal trends from 2000 through 2050. *Ophthalmology*. 2016;123(5):1036–1042.
  3. Sankaridurg P, Tahhan N, Kandel H, et al. IMI impact of myopia. *Invest Ophthalmol Vis Sci*. 2021;62(5):2.
  4. Flitcroft DI, He M, Jonas JB, et al. IMI - Defining and classifying myopia: a proposed set of standards for clinical and epidemiologic studies. *Invest Ophthalmol Vis Sci*. 2019;60(3):M20–M30.
  5. Jonas JB, Jonas RA, Bikbov MM, Wang YX, Panda-Jonas S. Myopia: histology, clinical features, and potential implications for the etiology of axial elongation. *Prog Retin Eye Res*. 2023;96:101156.
  6. Sebag J. Vitreous and vision degrading myodesopsia. *Prog Retin Eye Res*. 2020;79:100847.
  7. Nguyen JH, Nguyen-Cuu J, Mamou J, Routledge B, Yee KMP, Sebag J. Vitreous structure and visual function in myopic vitreopathy causing vision-degrading myodesopsia. *Am J Ophthalmol*. 2021;224:246–253.
  8. Sebag J. Posterior vitreous detachment. *Ophthalmology*. 2018;125(9):1384–1385.
  9. Hayashi K, Manabe SI, Hirata A, Yoshimura K. Posterior vitreous detachment in highly myopic patients. *Invest Ophthalmol Vis Sci*. 2020;61(4):33.
  10. Itakura H, Kishi S, Li D, Nitta K, Akiyama H. Vitreous changes in high myopia observed by swept-source optical coherence tomography. *Invest Ophthalmol Vis Sci*. 2014;55(3):1447–1452.
  11. Takahashi H, Tanaka N, Shinohara K, et al. Ultra-widefield optical coherence tomographic imaging of posterior vitreous in eyes with high myopia. *Am J Ophthalmol*. 2019;206:102–112.
  12. Abraham JR, Ehlers JP. Posterior vitreous detachment: methods for detection. *Ophthalmol Retina*. 2020;4(2):119–121.
  13. Moon SY, Park SP, Kim YK. Evaluation of posterior vitreous detachment using ultrasonography and optical coherence tomography. *Acta Ophthalmol*. 2020;98(1):e29–e35.
  14. Höhn F, Mirshahi A, Hattenbach LO. Optical coherence tomography for diagnosis of posterior vitreous detachment at the macular region. *Eur J Ophthalmol*. 2009;19(3):442–447.
  15. Láíns I, Wang JC, Cui Y, et al. Retinal applications of swept source optical coherence tomography (OCT) and optical coherence tomography angiography (OCTA). *Prog Retin Eye Res*. 2021;84:100951.
  16. Hwang ES, Kraker JA, Griffin KJ, Sebag J, Weinberg DV, Kim JE. Accuracy of spectral-domain OCT of the macula for detection of complete posterior vitreous detachment. *Ophthalmol Retina*. 2020;4(2):148–153.
  17. Tsukahara M, Mori K, Gehlbach PL, Mori K. Posterior vitreous detachment as observed by wide-angle OCT imaging. *Ophthalmology*. 2018;125(9):1372–1383.
  18. Hayashi A, Ito Y, Takatsudo Y, Hara N, Gehlbach PL, Mori K. Posterior vitreous detachment in normal healthy subjects younger than age twenty. *Invest Ophthalmol Vis Sci*. 2021;62(13):19.
  19. Mamou J, Wa CA, Yee KM, et al. Ultrasound-based quantification of vitreous floaters correlates with contrast sensitivity and quality of life. *Invest Ophthalmol Vis Sci*. 2015;56(3):1611–1617.
  20. Garcia GA, Khoshnevis M, Yee KMP, Nguyen-Cuu J, Nguyen JH, Sebag J. Degradation of contrast sensitivity function following posterior vitreous detachment. *Am J Ophthalmol*. 2016;172:7–12.
  21. Garcia GA, Khoshnevis M, Yee KMP, et al. The effects of aging vitreous on contrast sensitivity function. *Graefes Arch Clin Exp Ophthalmol*. 2018;256(5):919–925.
  22. Mano F, LoBue SA, Eno A, Chang KC, Mano T. Impact of posterior vitreous detachment on contrast sensitivity in patients with multifocal intraocular lens. *Graefes Arch Clin Exp Ophthalmol*. 2020;258(8):1709–1716.
  23. Ohno-Matsui K, Wu PC, Yamashiro K, et al. IMI Pathologic Myopia. *Invest Ophthalmol Vis Sci*. 2021;62(5):5.
  24. Ohno-Matsui K, Kawasaki R, Jonas JB, et al. International photographic classification and grading system for myopic maculopathy. *Am J Ophthalmol*. 2015;159(5):877–83.e7.
  25. Maniglia M, Thurman SM, Seitz AR, Davey PG. Effect of varying levels of glare on contrast sensitivity measurements of young healthy individuals under photopic and mesopic vision. *Front Psychol*. 2018;9:899.
  26. Lin M, Zhou H, Hu Z, Huang J, Lu F, Hu L. Comparison of small incision lenticule extraction and transepithelial photorefractive keratectomy in terms of visual quality in myopia patients. *Acta Ophthalmol*. 2021;99(8):e1289–e1296.
  27. Takmaz T, Genç I, Yildiz Y, Can I. Ocular wavefront analysis and contrast sensitivity in eyes implanted with AcrySof IQ or AcrySof

- Natural intraocular lenses. *Acta Ophthalmol.* 2009;87(7):759–763.
28. Applegate RA, Howland HC, Sharp RP, Cottingham AJ, Yee RW. Corneal aberrations and visual performance after radial keratotomy. *J Refract Surg.* 1998;14(4):397–407.
  29. Martínez-Roda JA, Vilaseca M, Ondategui JC, et al. Optical quality and intraocular scattering in a healthy young population. *Clin Exp Optom.* 2011;94(2):223–229.
  30. Adam CR, Shrier E, Ding Y, Glazman S, Bodis-Wollner I. Correlation of inner retinal thickness evaluated by spectral-domain optical coherence tomography and contrast sensitivity in Parkinson disease. *J Neuroophthalmol.* 2013;33(2):137–142.
  31. Mwanza JC, Oakley JD, Budenz DL, Chang RT, Knight OJ, Feuer WJ. Macular ganglion cell-inner plexiform layer: automated detection and thickness reproducibility with spectral domain-optical coherence tomography in glaucoma. *Invest Ophthalmol Vis Sci.* 2011;52(11):8323–8329.
  32. Wu H, Zhang G, Shen M, et al. Assessment of choroidal vascularity and choriocapillaris blood perfusion in anisomyopic adults by SS-OCT/OCTA. *Invest Ophthalmol Vis Sci.* 2021;62(1):8.
  33. Gillespie-Gallery H, Konstantakopoulou E, Harlow JA, Barbur JL. Capturing age-related changes in functional contrast sensitivity with decreasing light levels in monocular and binocular vision. *Invest Ophthalmol Vis Sci.* 2013;54(9):6093–6103.
  34. Shao L, Zhang C, Dong L, Zhou WD, Zhang RH, Wei WB. Prevalence and associations of vitreomacular traction: the Beijing Eye Study. *Int J Gen Med.* 2021;14:7059–7064.
  35. Ankamah E, Green-Gomez M, Roche W, et al. Impact of symptomatic vitreous degeneration on photopic and mesopic contrast thresholds. *Clin Exp Optom.* 2022;105(6):609–616.
  36. Young LK, Liversedge SP, Love GD, Myers RM, Smithson HE. Not all aberrations are equal: reading impairment depends on aberration type and magnitude. *J Vis.* 2011;11(13):20.
  37. Nguyen JH, Yee KM, Sadun AA, Sebag J. Quantifying visual dysfunction and the response to surgery in macular pucker. *Ophthalmology.* 2016;123(7):1500–1510.
  38. Ye C, Ng PK, Jhanji V. Optical quality assessment in normal and forme fruste keratoconus eyes with a double-pass system: a comparison and variability study. *Br J Ophthalmol.* 2014;98(11):1478–1483.
  39. Puell MC, Palomo-Álvarez C, Pérez-Carrasco MJ. Macular inner retinal layer thickness in relation to photopic and mesopic contrast sensitivity in healthy young and older subjects. *Invest Ophthalmol Vis Sci.* 2018;59(13):5487–5493.
  40. Hertenstein H, Bach M, Gross NJ, Beisse F. Marked dissociation of photopic and mesopic contrast sensitivity even in normal observers. *Graefes Arch Clin Exp Ophthalmol.* 2016;254(2):373–384.